Testing the Clausius-Clapeyron constraint on the aerosol-induced changes in mean and extreme precipitation

Gang Chen,[1] Yi Ming,[2] Noah D. Singer,[1] and Jian Lu[3,4]

Received 7 December 2010; revised 19 January 2011; accepted 28 January 2011; published 25 February 2011.

[1] The impacts of aerosol and greenhouse gas forcing of the 20th century on the climatological mean and extremes of precipitation are compared in an atmospheric GCM with improved parameterizations of aerosol direct and indirect effects. In spite of different forcing patterns, the thermodynamic effects of aerosol cooling and greenhouse gas warming on the zonally averaged precipitation have similar latitudinal patterns but opposite signs, plausibly due to the effects of temperature on atmospheric water vapor content and moisture flux. The fractional thermodynamic change, for both the moisture convergence in mid- and high latitudes and precipitation extremes at all latitudes, scales linearly with the abundance of atmospheric moisture at a rate of ~5%/K, somewhat less than the expectation from the Clausius-Clapeyron relation. **Citation:** Chen, G., Y. Ming, N. D. Singer, and J. Lu (2011), Testing the Clausius-Clapeyron constraint on the aerosol-induced changes in mean and extreme precipitation, *Geophys. Res. Lett.*, *38*, L04807, doi:10.1029/2010GL046435.

1. Introduction

[2] Substantial progress has been made in recent years in understanding the impacts of global warming on the mean and extreme precipitation. In the Coupled Model Intercomparison Project phase 3 (CMIP3) models, the mean precipitation in the 21st century is projected to increase in the tropics, mid- and high latitudes and decrease in the subtropics [e.g., *Emori and Brown*, 2005; *Held and Soden*, 2006; *Lorenz and DeWeaver*, 2007], yet the precipitation extremes are projected to intensify nearly at all latitudes with increasing greenhouse gas forcing [e.g., *Emori and Brown*, 2005; *O'Gorman and Schneider*, 2009; *Sugiyama et al.*, 2010].

[3] The increase in precipitation has been largely attributed to the expected increase in the water vapor-holding capacity of the atmosphere with global warming. However, the pace of the fractional increase in mean precipitation is much slower than the expected increase in saturation pressure of water vapor with temperature as described in the Clausius-Clapeyron (CC) relation (~7%/K). The difference has been attributed to the weakening of convective mass flux or the weakening of the tropical circulation in the greenhouse gas warming experiments [e.g., *Held and Soden*, 2006]. If the effect of atmospheric circulation change on precipitation can be separated, the remaining thermodynamic change in precipitation should follow the CC relation better. Here we test to what extent the CC relation can explain the thermodynamic change in precipitation simulated in an atmospheric GCM under different greenhouse gas and aerosol forcings.

[4] It is noteworthy that precipitation extremes predicted by climate models follow the CC relation better than the mean precipitation [*Allen and Ingram*, 2002; *Pall et al.*, 2007]. While the precipitation extremes depend on the moisture supply to the weather systems locally and over a short period of time, the mean precipitation is limited by the global and time mean moisture transport. In the time mean, the moisture transport equals precipitation minus evaporation ($P - E$), and therefore, the quantity relevant to the CC relation is $P - E$ rather than precipitation itself [*Held and Soden*, 2006].

[5] Relatively fewer studies have separated the thermodynamic and dynamic impacts of aerosols on precipitation. Aerosols can impact precipitation through complex aerosol-cloud-climate interactions. Roughly speaking, aerosols cool the surface in opposite to greenhouse gas warming. It is then expected that aerosols can alter the mean and extreme precipitation through changes in atmospheric moisture supply to weather systems through the CC relation. Recently in an atmospheric GCM with improved parameterizations of aerosol direct and indirect effects, Y. Ming et al. (Aerosol-induced changes in boreal winter extratropical circulation, submitted to Journal of Climate, 2010) argued that one can understand the variations in zonal-mean extratropical precipitation minus evaporation ($P - E$) largely from global-mean temperature change.

[6] While CO_2 is generally assumed to be well mixed in the atmosphere, aerosols are more influenced by surface emission sources, which would be important for regional climate change. For example, GCM experiments suggest that interhemispherically asymmetric cooling/heating can shift the position of the intertropical convergence zone (ITCZ) with a direct consequence on monsoon [*Chen and Ramaswamy*, 1996; *Rotstayn and Lohmann*, 2002; *Broccoli et al.*, 2006; *Ming and Ramaswamy*, 2009]. The shift of the ITCZ due to aerosol cooling indicates a dynamic change in precipitation different from the effect of greenhouse gas warming.

[7] In this paper, we compare the precipitation changes induced by greenhouse gas and aerosol forcing with an atmospheric GCM. We first separate the dynamic and thermodynamic components in the total precipitation change using an empirical method of *Emori and Brown* [2005], and

[1]Department of Earth and Atmospheric Sciences, Cornell University, Ithaca, New York, USA.
[2]Geophysical Fluid Dynamics Laboratory, NOAA, Princeton, New Jersey, USA.
[3]Center for Ocean-Land-Atmosphere Studies, Calverton, Maryland, USA.
[4]Department of Atmospheric, Oceanic and Earth Sciences, George Mason University, Fairfax, Virginia, USA.

0094-8276/11/2010GL046435

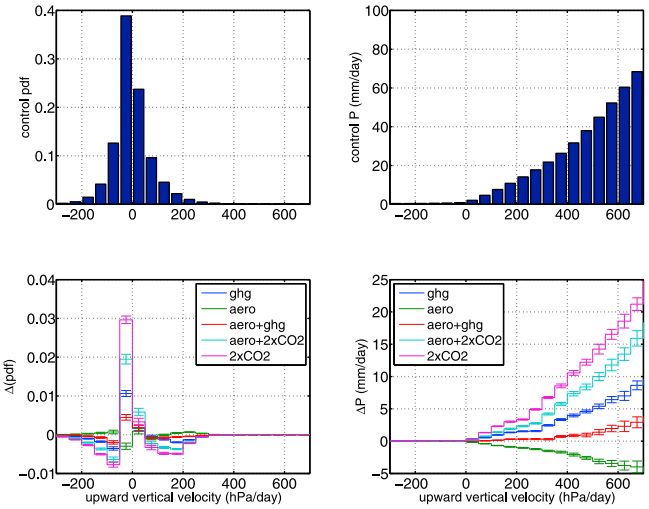

Figure 1. The globally averaged (left) probability distribution function (PDF) of daily upward vertical velocity at 500 hPa and (right) the composite daily precipitation in each vertical velocity bin. (top) The control simulation and (bottom) the changes in the perturbed experiments. Error bars denote the 95% confidence levels in t-tests.

then compare the thermodynamic changes with the CC relation.

2. Model and Method

[8] We examine the changes in precipitation in an atmospheric GCM, GFDL AM2.1, coupled with a slab (mixed-layer) ocean model described by *Ming and Ramaswamy* [2009]. The model utilizes the newly developed prognostic scheme for cloud condensation nuclei (CCN), which explicitly parameterizes dynamic and microphysical processes in aerosol-cloud interactions [*Ming et al.*, 2006, 2007]. Five perturbation cases were created by subjecting a pre-industrial control (CTRL) to the forcings: (1) AERO, (2) GHG, (3) AERO + GHG, (4) AERO + 2xCO_2, and (5) 2xCO_2, where the notations denote present-day aerosols (AERO), present-day radiatively active gases (GHG), and a doubling of pre-industrial CO_2 concentration (2xCO_2). 40-year daily outputs from 80-year model integrations are analyzed.

[9] Dynamic and thermodynamic changes in precipitation in the five perturbation experiments are separated using the method of *Emori and Brown* [2005]. The mid-tropospheric (500 hPa) daily vertical velocity, ω, is used as a proxy for the dynamic control of the atmosphere on precipitation. The daily change in vertical velocity at each grid point represents the strength and phase of weather systems passing the point of interest. This is well correlated with precipitation rate in most regions, and we have excluded as done by *Emori and Brown* [2005] some subtropical regions, where the lower tropospheric vertical velocity is likely a better proxy for the circulation control on precipitation.

[10] First, an empirical relationship $P(\omega)$ between precipitation intensity and the pressure velocity is constructed by binning the precipitation intensity with respect to the values of upward vertical velocity. 40 bins are evenly divided from −1000 hPa/day to 1000 hPa/day with an increment of $d\omega$ = 50 hPa/day. The probability density function of omega can be estimated on the same bins and designated as $\Omega(\omega)$. Both $P(\omega)$ and $\Omega(\omega)$ are calculated locally at each grid point, and $P(\omega)$ represents local average precipitation rate for all the weather events categorized from ω to $\omega + d\omega$.

[11] The annual mean precipitation at each grid point can be described as

$$\overline{P} = \int_{-\infty}^{\infty} P(\omega)\Omega(\omega)d\omega \tag{1}$$

Then the change of annual mean precipitation in the perturbed runs can be described as

$$\delta\overline{P} = \int_{-\infty}^{\infty} P(\omega)\delta\Omega(\omega)d\omega + \int_{-\infty}^{\infty} \delta P(\omega)\Omega(\omega)d\omega + \int_{-\infty}^{\infty} \delta P(\omega)\delta\Omega(\omega)d\omega \tag{2}$$

where the first term on the RHS denotes the precipitation change due to the vertical velocity (dynamic) change. The second term denotes the precipitation change due to the change of expected precipitation for given vertical velocity. This is controlled by the precipitable water vapor in the atmosphere, termed as a thermodynamic change. The third term is a nonlinear covariance term.

[12] Using the statistical relationship $P = P(\omega)$, the change of precipitation extreme, defined as the eth (high) percentile of precipitation P^e, can be expressed as,

$$\delta P^e = \frac{\partial p(\omega)}{\partial \omega}\delta\omega^e + \delta P(\omega^e) + \delta\frac{\partial P(\omega)}{\partial \omega}\delta\omega^e \tag{3}$$

where ω^e is the vertical velocity value at which the eth percentile of precipitation P^e occurs and can be obtained by inverting the statistical relationship $\omega^e = P^{-1}(P^e)$. Again, the three terms on the RHS represent dynamic, thermodynamic, and covariance changes in precipitation, respectively. In particular, the second term denotes the change in the expected precipitation for given vertical velocity, and is controlled by atmospheric moisture.

[13] As discussed in the introduction, if the statistics of the intensity and frequency of weather systems remain unchanged (i.e., no dynamic change), the fractional change in $P - E$ or P^e should vary with the fractional change in the abundance of atmospheric moisture. Further, if the relative humidity of the atmosphere does not change, the fractional change of atmospheric moisture scales as the CC relation (~7%/K).

3. Results

[14] Figure 1 shows the global mean probability density function (PDF) of daily upward vertical velocity (negative pressure velocity at 500 hPa) and the composite daily precipitation in each velocity bin. In the control simulation, the frequency of vertical velocity peaks near zero and the precipitation intensity increases monotonically with stronger updraft. As the surface temperature increases sequentially (i.e., experiments AERO, AERO + GHG, GHG, AERO +

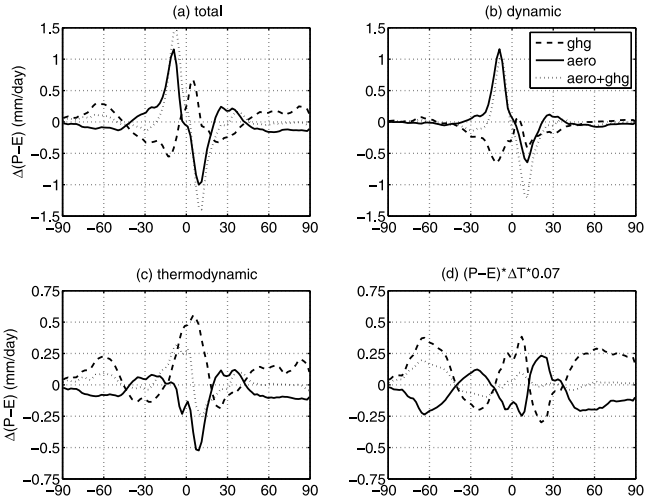

Figure 2. The zonally averaged change of precipitation minus evaporation ($P - E$): (a) total change, (b) dynamic change, (c) thermodynamic change, (d) Clausius-Clapeyron scaling.

$2xCO_2$, and $2xCO_2$, see Figure S1 of the auxiliary material for details),[1] the global mean vertical velocity is weakened due to the increased frequency of weaker vertical motion at the expense of stronger updraft and downdraft, and the precipitation rate in each upward velocity bin is successively enhanced, as expected from the thermodynamic control.

[15] Figure 2 compares the mean $P - E$ change in three experiments: AERO, GHG, and AERO + GHG. The total change in $P - E$ is decomposed into dynamic and thermodynamic changes as outlined in Section 2. Both contribute to tropical precipitation change, and the thermodynamic component explains most of the extratropical change, as found in the response to global warming in CMIP3 models [*Emori and Brown*, 2005]. The dynamic changes are different between the AERO and GHG runs. The ITCZ shifts southward in response to the aerosol forcing, due to more cooling in the NH and a net cross-equatorial energy transport [*Ming and Ramaswamy*, 2009]. The dynamic effect of greenhouse gas warming is a reduction in the tropical circulation and convective mass flux [*Held and Soden*, 2006], and as a consequence, the dynamically-induced precipitation change in the tropics is reduced substantially. It is particularly noteworthy that the thermodynamic changes in the mean $P - E$ induced by AERO and GHG are almost mirror image of each other (Figures 2c and 2d), implicative of a considerable thermodynamic constraint of temperature on the latitudinal distribution of the hydrological cycle. Other than the small nonlinearity noted by *Ming and Ramaswamy* [2009], the precipitation responses to greenhouse gas and aerosol forcings are approximately additive.

[16] Figure 3 compares the changes of precipitation extreme, defined as the 99th percentile of daily precipitation (approximately the annual 4th largest precipitation rate), for the same three experiments. Again, we find that most of extratropical changes are due to changes in thermodynamics, and tropical changes are the results of both dynamics and thermodynamics, as for GHG-induced global warming [*Emori and Brown*, 2005]. The dynamic contribution to precipitation extremes in GHG shows an increase at the equator, and a decrease at about 20N or 20S. By contrast, an increase in precipitation extremes is found for the AERO case at about 20N or 20S. Interestingly, the precipitation extreme does not change much at 0-15N despite that the mean precipitation is dynamically reduced. On the other hand, the thermodynamic components due to AERO and GHG tend to be opposite to each other with the latitudinal distributions resembling their corresponding surface temperature changes (Figure S1). Again, the CC relation seems to exert a strong constraint to the thermodynamic changes in precipitation extremes for both AERO and GHG. As by *Emori and Brown* [2005], we found that the covariance term is negligible for the mean and extreme precipitation in most regions (not shown).

[17] To see how well the mean and extreme precipitation changes match the CC relation, we conduct the CC scaling for all of the five cases using the local mean surface temperature and the assumption of fixed relative humidity. Although this simple CC scaling relation accounts for considerable latitudinal distribution of the response in both mean (Figure 2d) and extreme (Figure 3d) precipitation, it overestimates the modeled thermodynamic response in the extratropics for both mean and extremes, and underestimates the mean thermodynamic response in the tropics. In Figure 4, we compare the fractional change of $P - E$ in mid-to-high latitudes (90-45S and 45-90N) with altered moisture convergence as a function of surface temperature through the CC scaling. Although not aligning along the 7%/K CC rate exactly, the fractional change of $P - E$ scales linearly with surface temperature at a rate of ~5%/K. Remarkably, a similar scaling rate is also found in the fractional change in precipitation extremes in the extratropics and the thermodynamic components in the tropics. These results consistently demonstrate the significance of the thermodynamic constraint on the precipitation response to climate change, especially over the extratropical regions. The

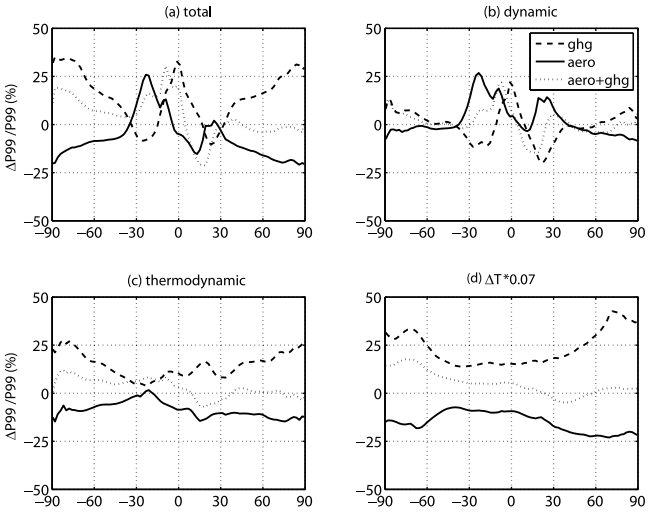

Figure 3. The zonally averaged fractional change of the 99th percentile of daily precipitation (approximately the annual 4th largest precipitation rate): (a) total change, (b) dynamic change, (c) thermodynamic change, (d) Clausius-Clapeyron scaling.

[1] Auxiliary materials are available in the HTML. doi:10.1029/2010GL046435.

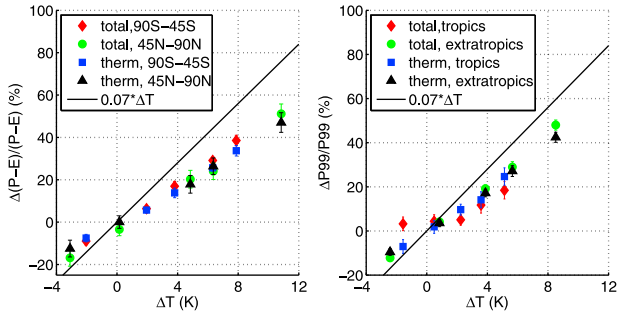

Figure 4. The total and thermodynamic changes of mean and extreme precipitation in percentage over different regions versus surface temperature changes: (left) the mean $P - E$ for 90S-45S and 45N-90N, (right) the 99th percentile of daily precipitation for tropics and extratropics. Error bars denote the 95% confidence levels in t-tests.

total change in precipitation extremes in the tropics is sensitive to both the percentile used and the degree of surface warming (not shown), likely due to the dynamical changes associated with AREO and GHG.

4. Conclusion and Discussion

[18] We have compared the impacts of the climate forcing by aerosols versus greenhouse gases on precipitation in an atmospheric GCM with a slab mixed layer ocean. The dynamic changes, mostly confined in the tropics, are characterized by a southward shift of the ITCZ under inhomogeneous aerosol cooling, in contrast to the weakening tropical circulation with homogeneous greenhouse gas warming. Despite of the spatial inhomogeneity, aerosols exert thermodynamic impacts on zonally averaged mean and extreme precipitation similar to greenhouse gases except for opposite signs. This is attributed physically to similar thermodynamic effects on atmospheric water vapor content and moisture flux through the CC relation. The effects of the two forcings are largely canceled when both of them are imposed, and a transient simulation is needed to assess the contributions to the historical temperature and precipitation changes.

[19] The fractional thermodynamic change in the $P - E$ in mid- and high latitudes and precipitation extremes at all latitudes, scales linearly with the surface temperature change due to aerosol cooling or greenhouse gas warming, as expected from the altered moisture held in the atmosphere. This provides additional confidence to the thermodynamic interpretation of atmospheric hydrological cycle response to climate change. The rate of change is however ~5%/K, somewhat less than the expectation from the CC relation, as found in the precipitation changes under global warming [*Lorenz and DeWeaver*, 2007; *O'Gorman and Schneider*, 2009]. The reason for the sub-CC behavior is the topic of on-going investigation and the result will be reported elsewhere.

[20] **Acknowledgments.** We thank anonymous reviewers for their constructive comments that greatly improved our paper.

[21] Geoffrey S. Tyndall thanks Beate Leipert and an anonymous reviewer.

References

Allen, M. R., and W. J. Ingram (2002), Constraints on future changes in climate and the hydrologic cycle, *Nature*, *419*, 224–232.

Broccoli, A. J., K. A. Dahl, and R. J. Stouffer (2006), Response of the ITCZ to Northern Hemisphere cooling, *Geophys. Res. Lett.*, *33*, L01702, doi:10.1029/2005GL024546.

Chen, C. T., and V. Ramaswamy (1996), Sensitivity of simulated global climate to perturbations in low cloud microphysical properties. Part II: Spatially localized perturbations, *J. Clim.*, *9*, 2788–2801.

Emori, S., and S. J. Brown (2005), Dynamic and thermodynamic changes in mean and extreme precipitation under changed climate, *Geophys. Res. Lett.*, *32*, L17706, doi:10.1029/2005GL023272.

Held, I. M., and B. J. Soden (2006), Robust responses of the hydrological cycle to global warming, *J. Clim.*, *19*, 5686–5699.

Lorenz, D. J., and E. DeWeaver (2007), The response of the extratropical hydrological cycle to global warming, *J. Clim.*, *20*, 3470–3484.

Ming, Y., and V. Ramaswamy (2009), Nonlinear climate and hydrological responses to aerosol effects, *J. Clim.*, *22*, 1329–1339, doi:10.1175/2008JCLI2362.1.

Ming, Y., V. Ramaswamy, L. J. Donner, and V. T. J. Phillips (2006), A new parameterization of cloud droplet activation applicable to general circulation models, *J. Atmos. Sci.*, *63*, 1348–1356.

Ming, Y., V. Ramaswamy, L. J. Donner, V. T. J. Phillips, S. A. Klein, P. A. Ginoux, and L. W. Horowitz (2007), Modeling the interactions between aerosols and liquid water clouds with a self-consistent cloud scheme in a general circulation model, *J. Atmos. Sci.*, *64*, 1189–1209.

O'Gorman, P. A., and T. Schneider (2009), The physical basis for increases in precipitation extremes in simulations of 21st-century climate change, *Proc. Natl. Acad. Sci. U. S. A.*, *106*, 14,773–14,777.

Pall, P., M. R. Allen, and D. A. Stone (2007), Testing the Clausius-Clapeyron constraint on changes in extreme precipitation under CO_2 warming, *Clim. Dyn.*, *28*, 351–363.

Rotstayn, L. D., and U. Lohmann (2002), Tropical rainfall trends and the indirect aerosol effect, *J. Clim.*, *15*, 2103–2116.

Sugiyama, M., H. Shiogama, and S. Emori (2010), Precipitation extreme changes exceeding moisture content increases in MIROC and IPCC climate models, *Proc. Natl. Acad. Sci. U. S. A.*, *107*, 571–575.

G. Chen and N. D. Singer, Department of Earth and Atmospheric Sciences, Cornell University, Ithaca, NY 14853, USA. (gc352@cornell.edu)

J. Lu, Center for Ocean-Land-Atmosphere Studies, 4041 Powder Mill Rd., Calverton, MD 20705, USA.

Y. Ming, Geophysical Fluid Dynamics Laboratory, NOAA, 201 Forrestal Rd., Princeton, NJ 08540, USA.